Reduced Photoconductivity Observed by Time-Resolved Terahertz Spectroscopy in Metal Nanofilms with and without Adhesion Layers

Brian G. Alberding,[1] Gary P. Kushto,[2] Paul A. Lane,[2] and Edwin J. Heilweil[*,1]

[1]Radiation Physics Division, National Institute of Standards and Technology, 100 Bureau Drive, Gaithersburg, MD 20899

[2]Optical Sciences Division, US Naval Research Laboratory, Washington, D.C. 20375

Supporting Information

Methods

a. Materials

Gold, titanium, and chromium were obtained commercially and used as recieved.[1] Hydrochloric acid and nitric acid were reagent grade and used as received. The reference silicon (Si) wafer was purchased from University Wafer (ID 2018). It was high resistivity (> 10 000 ohm cm), <100> orientation, double side polished and 280 μm thick. Fused quartz substrates were purchased from GM Associates, Inc.

b. Fabrication and Morphology of Metal Films

The thin metal films were prepared by electron beam deposition onto clean fused quartz substrates within a vacuum chamber held at 667 Pa (5 x 10^{-7} torr). Substrates were masked to give a film area of ~2.0 cm x 2.5 cm and multiple equivalent samples were prepared side-by-side during the same deposition. A quartz crystal microbalance was used to monitor the rate of deposition and determine the film thickness of the metal layers. A sequential process was used to prepare the films with adhesion layers. In total, the metal film samples on fused quartz substrates included 8nm of gold (8nmAu), 8nm of gold with a 4 nm adhesion layer of either titanium or chromium (8nmAu/4nmTi or 8nmAu/4nmCr, respectively), and 8nm of titanium (8nmTi). AFM imaging was done for 8nmAu, 8nmAu/4nmCr, and 8nmAu4nmTi in ambient using an Agilent 5500 Atomic Force Microscope in non-contact/tapping mode. The cantilever was highly doped silicon with a tip radius of 8 ±2 nm.

A sample was also prepared by exposing a duplicate sample of the 8nmAu/4nmCr film to aqua regia to remove the gold layer. This was done by dipping the film in aqua regia for 1 minute followed by sequentially rinsing with distilled water and ethanol and then drying under a stream of compressed air. The black film that remained following this treatment is denoted 4nmCr in the text, but is most likely described as Cr_2O_3, the most stable form of oxidized chromium and known to form when thin films of chromium metal are exposed to ambient conditions.[2] A similar Au-removal procedure was attempted for the 8nmAu/4nmTi film however the treatment with aqua regia resulted in complete removal of the metal film.

c. Optical Spectroscopy and Terahertz Spectroscopy

Transmission measurements between 300 nm and 1100 nm were made on the metal thin films using a PerkinElmer Lambda 2 UV-Vis spectrometer. For all samples, the absorbance was referenced to a blank spot on the sample substrate.

The apparatus for terahertz spectroscopy is based on an amplified femtosecond Ti:sapphire laser system (Coherent MIRA seed and Legend regenerative amplifier) that operates at 1 KHz repetition rate.[3] The amplified 800 nm pulse train (1.6 mJ/pulse and 40 fs full-width half-maximum pulse duration) is split into three arms for the visible pump, terahertz probe, and gated electro-optic detection. The first arm is directed down a delay stage and used for visible photoexcitation. (400 nm or 800 nm, beam diameter ~ 5 mm, FWHM ~ 50 fs, maximum 80 μJ/pulse). The second arm is directed down another delay stage and then onto a 1 mm thick zinc telluride (ZnTe) crystal to generate the terahertz frequency probe pulses by optical rectification. The generated probe pulses are then focused (~ 2 mm to 3 mm beam diameter) onto the sample by a pair of parabolic mirrors and transmitted through the sample. The third arm serves as the gate pulse for the electro-optic detection scheme. Here, the 800 nm gate pulses are attenuated and then recombined with the transmitted terahertz probe pulses in a 0.5 mm thick ZnTe detector crystal at various probe delay times to map out the terahertz pulse waveform. The electro-optic effect in the ZnTe detector crystal results in a depolarization of the 800 nm gate pulse that depends on the magnitude and sign of the electric field of the terahertz probe pulse. The resulting polarization in the 800 nm gate pulse is analyzed by a λ/4 wave plate and Wollaston prism and then collected by a pair of balanced silicon photodetectors using lock-in amplification (Stanford Research Systems, SR830).

Samples were mounted on an aperture larger than the terahertz and visible pump beam sizes and housed within a chamber purged with dry air to avoid absorption of the terahertz probe by atmospheric water. All measurements were done at room temperature. Electric field waveforms of the terahertz pulses are measured by scanning the probe delay time relative to the gate pulse. For THz-TDS measurements, 10 scans of the transmitted waveform through the sample and substrate were collected and averaged. To measure TRTS decay dynamics, the delay between the excitation and probe pulse is scanned, keeping the delay between the gate and probe pulses fixed at the position that gives the maximum electro-optic response. Ten sweeps of the pump scans were collected and averaged. For all samples, the excitation power used was 80 μJ/pulse, except for Si which was excited with 0.2 μJ/pulse.

d. THz Data Analysis

An increase in THz transmission after excitation corresponds to a decrease in photo-induced conductivity while a decrease in transmission indicates increased conductivity according to equation (S1),[4,5]

$$\Delta\sigma(t) = -\left(\frac{n_{THz}+1}{Z_0 d}\right)\left(\frac{\Delta E(t)}{E_0}\right) \qquad (S1)$$

where ΔE(t) is the differential electric field transmission measured at the peak of the terahertz waveform and pump-probe delay time, t, E_0 is the terahertz transmission through the unexcited sample, n_{THz} is the index of refraction of the substrate in the frequency range of the THz pulse (0.5 THz to 2.0 THz), Z_0 is the

permittivity of free space, d is the thickness of the photoexcited sample, and $\Delta\sigma(t)$ is the frequency-averaged real part of the photoconductivity.[4] It should be noted that this equation assumes the conductivity of the non-photoexcited sample is zero and has been routinely applied to thin film semiconductor samples. For the metallic thin film samples studied here, the conductivity of the non-photoexcited sample is non-zero and so it is more appropriate to consider equation (S2),[5]

$$-\frac{\Delta E(t)}{E_0} = \frac{Z_0 d \Delta\sigma(t)}{n_{THz} + 1 + Z_0 d \sigma_{ex}(t)} \qquad (S2)$$

where $\sigma_{ex}(t)$ is the frequency averaged real part of the photoconductivity for the photoexcited sample. In either case, the conductivity changes induced by the excitation pulse are proportional to the changes in electric field transmission and the sign of ΔE can be used to differentiate between metallic and semiconducting materials. To unambiguously determine the sign of $\Delta E/E_0$, we calibrate the lock-in amplifier phase (which indicates the sign of ΔE) using the known decreased transmission response from a high resistivity Si wafer.

To measure TDS waveforms, we scan the delay of the probe pulse relative to the gate pulse in the absence of the photoexcitation pulse. The TDS data were collected for the samples by acquiring ten probe pulse sweeps with averaging and comparing samples with blank spots on the same substrate scanned before each sample. Extraction of frequency-dependent conductivity from these data was performed using standard methods using equation S3,[6]

$$\boldsymbol{\sigma}(\omega) = \left(\frac{n_{THz} + 1}{Z_0 d}\right)\left(\frac{\boldsymbol{E_{substrate}(\omega)}}{\boldsymbol{E_{sample}(\omega)}} - 1\right) \qquad (S3)$$

where $\mathbf{E_{sample}(\omega)}$ and $\mathbf{E_{substrate}(\omega)}$ is the complex-valued Fourier transform of the terahertz electric field transmission through the sample and substrate, respectively, and $\boldsymbol{\sigma}(\omega)$ is the complex-valued photoconductivity.

Supplemental Figures

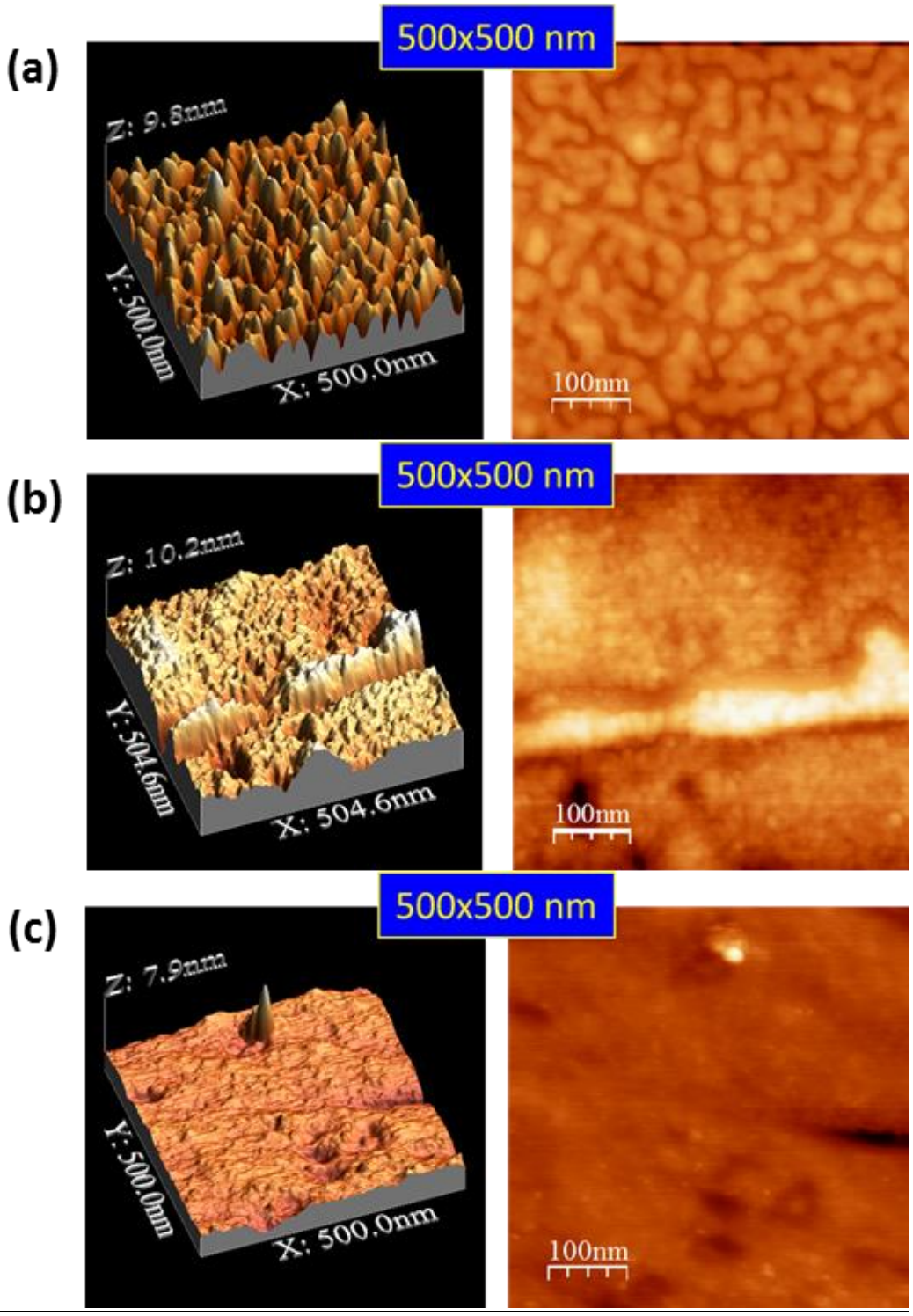

Figure S1: AFM images of a 500x500 nm scanning window for (a) 8nmAu with 1.66 nm root-mean squared (RMS) roughness (b) 8nmAu/4nmCr with 0.83 nm RMS roughness and (c) 8nmAu/4nmTi with 0.40 RMS roughness.

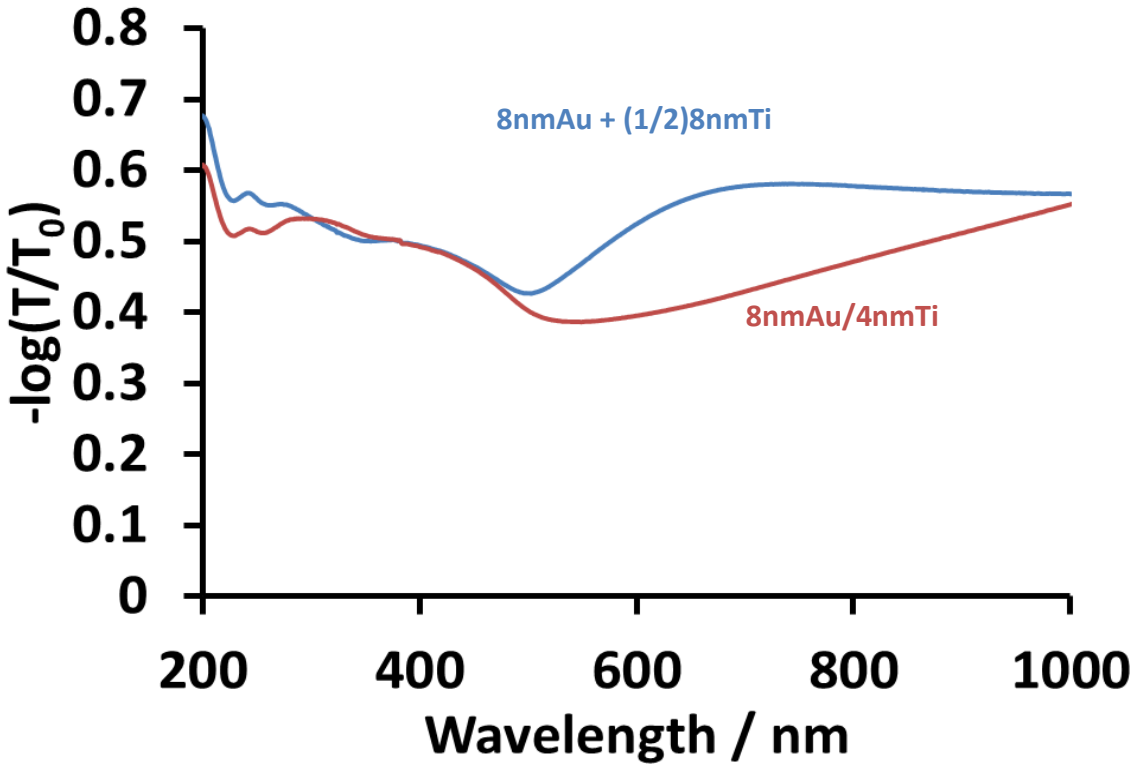

Figure S2: Comparison of UV-Visible transmission spectra for the 8nmAu/4nmTi film (red) and an approximated film derived from the sum of the 8nmAu film with ½ the 8nmTi film (blue). This result demonstrates that the 8nmAu/4nmTi film cannot be described by distinct Au and Ti absorptive layers.

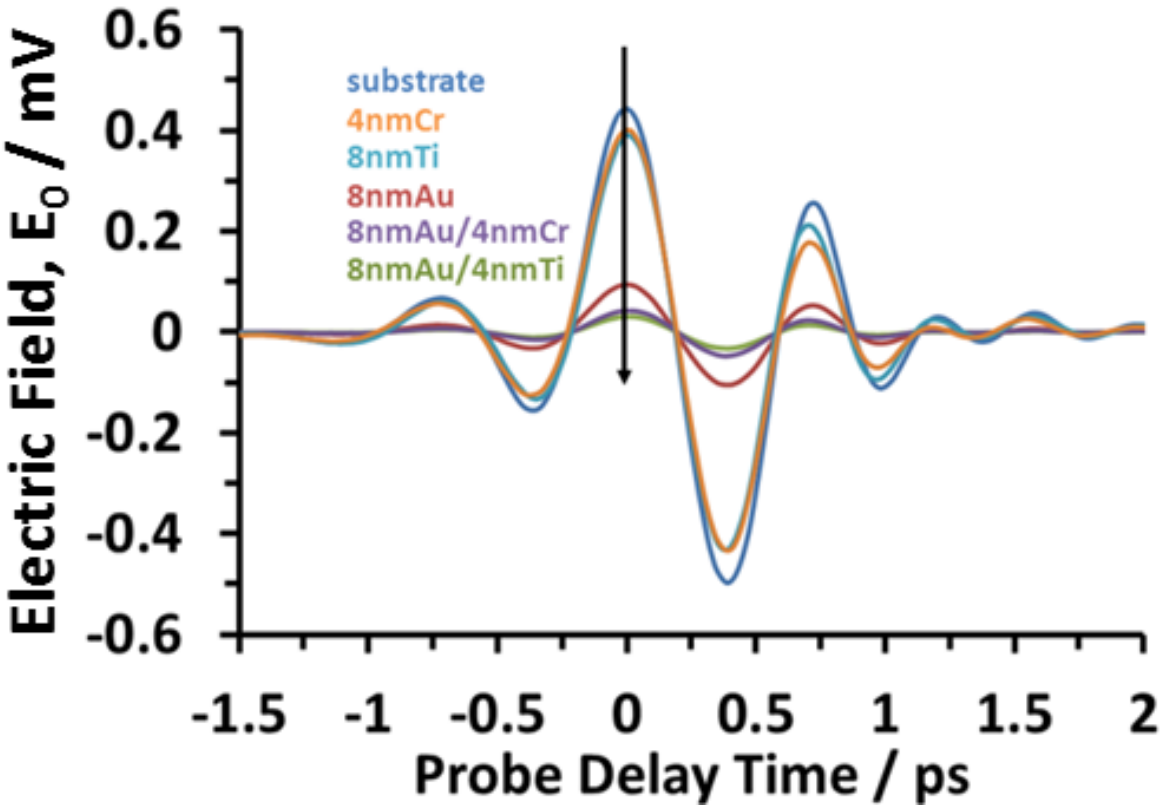

Figure S3: Terahertz probe pulse electric field transmission through each of the films compared to a representative substrate scan.

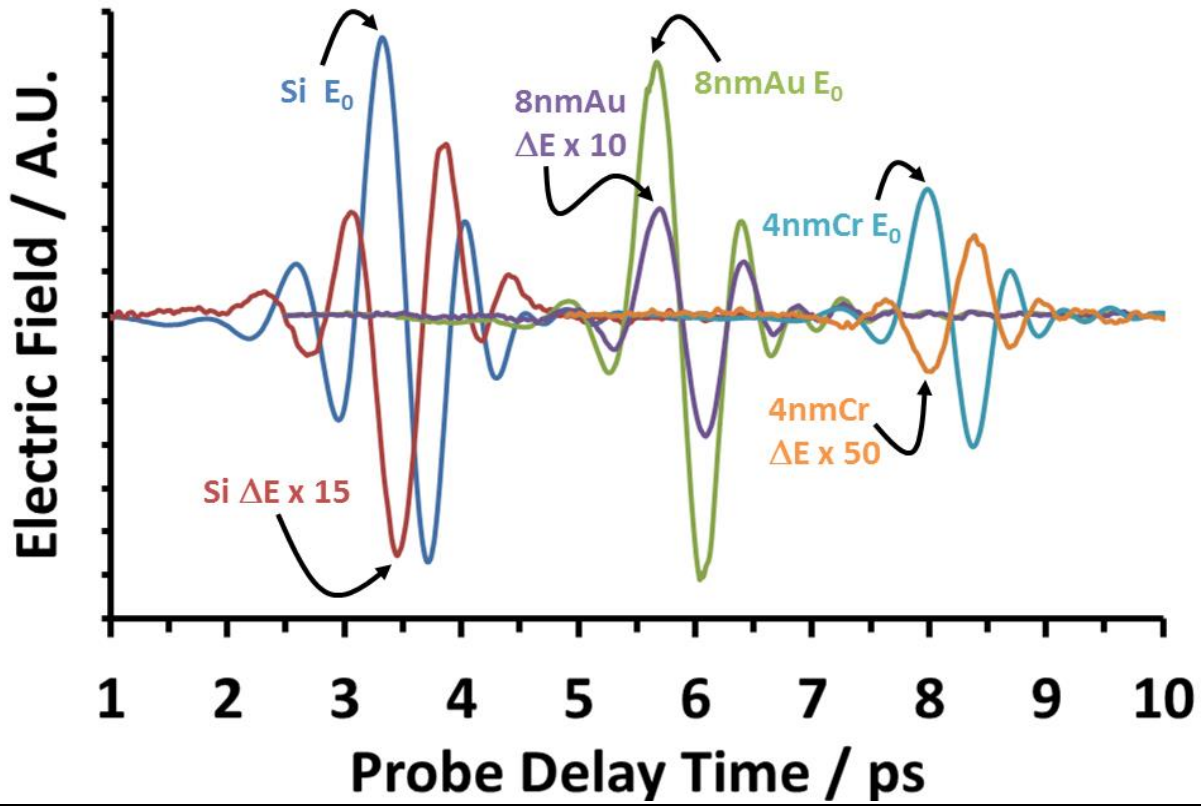

Figure S4: A comparison of the transient changes in the probe pulse electric field transmission, ΔE, following photoexcitation to the transmission of the terahertz electric field without photoexciation, E_0, for the Si, 8nmAu, and 4nmCr films, where the ΔE values have been adjusted by the indicated scaling factors relative to E_0 for clarity. The metallic gold film has the opposite sign of ΔE as the semiconductor samples. The films' probe pulse responses have been offset along the delay time axis for clarity.

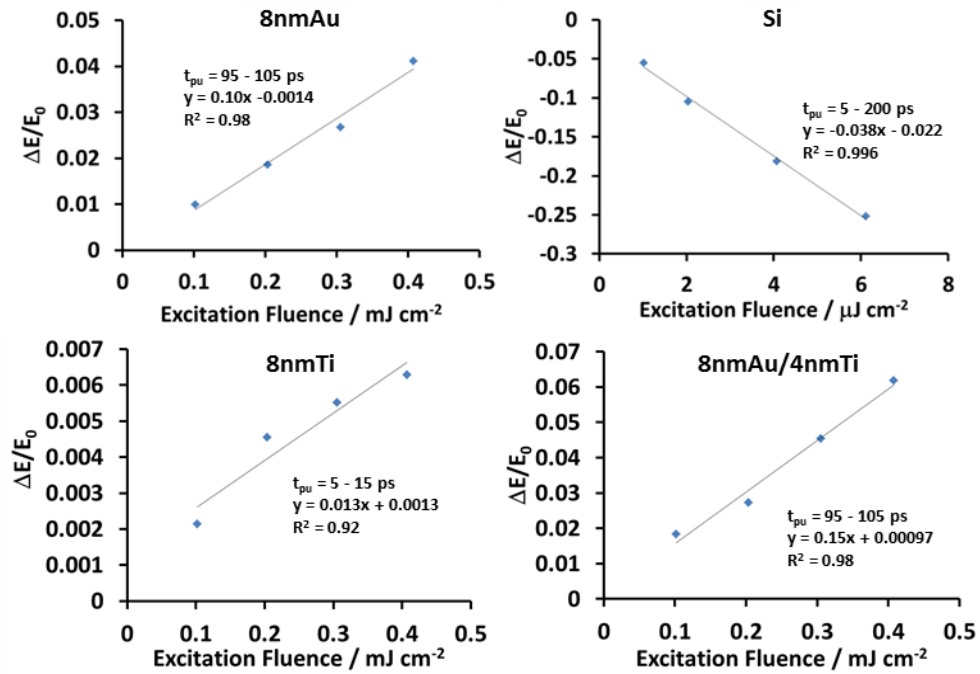

Figure S5: Excitation fluence dependence of the TRTS signal magnitudes, $\Delta E/E_0$, averaged over the indicated pump-probe delay times, t_{pu}.

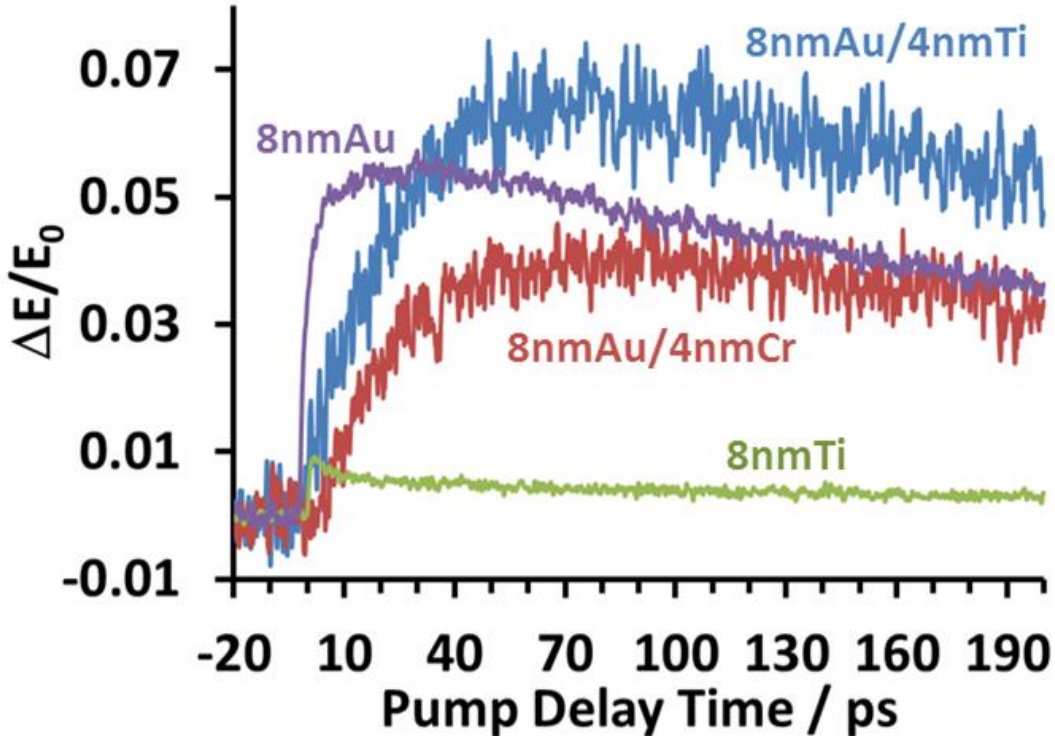

Figure S6: TRTS measurements of the 8nmAu (purple), 8nmTi (green), 8nmAu/4nmTi (blue), and 8nmAu/4nmCr (red) films following 400 nm excitation at room temperature.

References

(1) Certain commercial equipment or materials are identified in this paper to adequately specify the experimental procedures. In no case does the identification imply recommendation or endorsement by NIST, nor does it imply that the materials or equipment identified are necessarily the best available for the purpose.

(2) Julkarnain, M.; Hossain, J.; Sharif, K. S.; Khan, K. A. Temperature Effect on the Electrical Properties of Chromium Oxide (Cr_2O_3) Thin Films. *J. Optoelectron. Adv. Mater.* **2011**, *13* (5), 485–490.

(3) Esenturk, O.; Melinger, J. S.; Heilweil, E. J. Terahertz Mobility Measurements on Poly-3-Hexylthiophene Films: Device Comparison, Molecular Weight, and Film Processing Effects. *J. Appl. Phys.* **2008**, *103* (2), 023102.

(4) Nienhuys, H.-K.; Sundström, V. Intrinsic Complications in the Analysis of Optical-Pump, Terahertz Probe Experiments. *Phys. Rev. B* **2005**, *71* (23), 235110.

(5) Hegmann, F. A.; Ostroverkhova, O.; Cooke, D. G. Probing Organic Semiconductors with Terahertz Pulses. In *Photophysics of Molecular Materials*; Wiley-VCH: Weinheim, 2006; pp 367–428.

(6) Walther, M.; Cooke, D. G.; Sherstan, C.; Hajar, M.; Freeman, M. R.; Hegmann, F. A. Terahertz Conductivity of Thin Gold Films at the Metal-Insulator Percolation Transition. *Phys. Rev. B* **2007**, *76* (12), 125408.